JOC*Article*

Total Synthesis of Ustiloxin D and Considerations on the Origin of Selectivity of the Asymmetric Allylic Alkylation

Andrew M. Sawayama,[†] Hiroko Tanaka,[†] and Thomas J. Wandless*[,‡]

Department of Chemistry, Stanford University, Stanford, California 94305, and Department of Molecular Pharmacology, Stanford University, Stanford, California 94305

wandless@stanford.edu

Received July 6, 2004

As part of investigations into cell cycle checkpoint inhibitors, an asymmetric synthesis of the antimitotic natural product, ustiloxin D, has been completed. A salen−Al-catalyzed aldol reaction was employed to construct a chiral oxazoline **9** (99% yield, 98% ee) that served the dual purpose of installing the necessary 1,2-amino alcohol functionality as well as providing an efficient synthon for the requisite methylamino group at C9. The chiral aryl−alkyl ether was assembled using a Pd-catalyzed asymmetric allylic alkylation that notably delivered a product with stereochemistry opposite to that predicted by precedent. The linear tetrapeptide was subsequently cyclized to produce ustiloxin D. The mechanistic origin of the allylic alkylation selectivity was further investigated, and a working hypothesis for the origin of the observed stereoselectivity has been proposed.

Introduction

Iwasaki and co-workers isolated[1] ustiloxins A−D from the water extract of the fungus *Ustilaginoidea virens* growing on rice (Chart 1). This metabolite was reported to poison domestic animals that consumed the infected rice plant. In 1992, the structure of ustiloxin A was determined using a combination of X-ray crystallography, ^{1}H and ^{13}C NMR, and degradation studies. The structures of ustiloxins B−D were determined by comparison of their spectral properties and amino acid analyses in relation to ustiloxin A. Several years before, Edgar isolated phomopsins A and B as the principle mycotoxin from cultures of *Phomopsis leptostromiformis*.[2] Of significant economic impact to Australia and New Zealand, sheep, cattle, and horses that consumed lupin infected with this fungus developed severe liver damage. The constituent amino acids of phomopsin A were identified using degradation studies followed by extensive ^{1}H and ^{13}C NMR.[3] X-ray crystallographic studies confirmed the relative configuration of its eight stereocenters in 1986.[4]

Though the effects of these molecules on livestock are certainly important, we were more drawn to their mode of biological activity. Liver specimens of animals with lupinosis revealed metaphase-arrested cells. Confirming their role as an antimitotic agent, light-scattering experiments have demonstrated that the ustiloxins and phomopsins are potent microtubule depolymerizers both in vitro and in vivo.[5,6] Competitive binding has shown that this class of molecule binds to the same site as structur-

CHART 1. Ustiloxins and Phomopsins

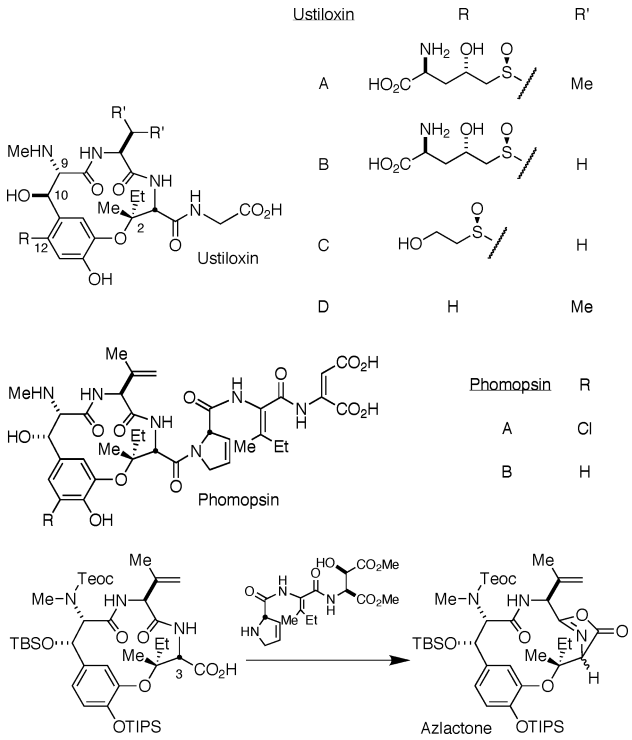

† Department of Chemistry.

‡ Department of Molecular Pharmacology.

(1) (a) Koiso, Y.; Natori, S.; Iwasaki, S.; Sato, S.; Sonoda, R.; Fujita, Y.; Yaegashi, H.; Sato, Z. *Tetrahedron Lett.* **1992**, *33*, 4157−4160. (b) Koiso, Y.; Li, Y.; Iwasaki, S. *J. Antibiot.* **1994**, *47*, 765−773. (c) Koiso, Y.; Morisaki, N.; Yamashita, Y.; Mitsui, Y.; Shirai, R.; Hashimoto, Y.; Iwasaki, S. *J. Antibiot.* **1998**, *51*, 418−422.

(2) Culvenor, C. C. J.; Beck, A. B.; Clarke, M.; Cockrum, P. A.; Edjar, J. A.; Frahn, J. L.; Jago, M. W.; Lanigan, G. W.; Pane, A. L.; Peterson, J. E.; Smith, L. W.; White, R. R. *Aust. J. Biol. Sci*. **1977**, *30*, 269−277.

(3) Culvenor, C. C. J.; Edgar, J. A.; MacKay, M. F. *Tetrahedron* **1989**, *45*, 2351−2372.

(4) MacKay, M. F.; Van Donkelaar, A.; Culvenor, C. C. J. *J. Chem. Soc., Chem. Commun.* **1986**, 1219−1221.

(5) Ludueña, R. F.; Roach, M. C.; Prasad, V.; Banerjee, J.; Koiso, Y.; Li, Y.; Iwasaki, S. *Biochem. Pharmacol.* **1994**, *47*, 1593−1599.

(6) Tönsing, E. M.; Steyn, P. S.; Osborn, M.; Weber, K. *Eur. J. Cell. Biol.* **1984**, *35*, 156−164.

10.1021/jo048854f CCC: $27.50
Published on Web 11/11/2004

ally unrelated rhizoxin and dolastatin 10,[7] overlapping somewhat with the vinca alkaloid binding site. As part of the larger goal of understanding the mammalian spindle assembly checkpoint, we are pursuing the syntheses of these natural products and structurally related variants with the goal of dissecting the cell signaling pathway by which the integrity of microtubules is monitored.

Structure−activity relationships in microtubule depolymerization assays indicate that the complex phomopsin A tripeptide side chain is not essential since ustiloxin D retains most of its antimitotic activity with a simple glycine side chain (IC_{50} = 2.4 vs 6.6 μM).[8] Furthermore, reduction and protection of the glycine acid does not even change activity by an order of magnitude.[8] Hydrogenation of phomopsin A to octahydrophomopsin A[9] had little effect as well. Other structural differences include the opposite stereochemistry at the C10 hydroxyl and chlorination of the hydroxytyrosine arene. These elements are most likely unnecessary features for microtubule depolymerization. However, the 13-membered macrocyclic motif, the hydroxytyrosine *N*-methylation, and the (*R*)-configuration of the C2 ether are preserved throughout each family member.

This family of molecules has attracted the interest of many groups. Semisyntheses of analogues,[8,10] pared down ustiloxin model compounds,[11] and the synthesis of the chiral sulfoxide C12 substituent[12] have been reported. Of particular note, the Joullié group completed the first total synthesis of ustiloxin D[13] using a strategy by which the C2 ether was assembled using nucleophilic aromatic substitution and the C9/C10 amino alcohol was constructed by Sharpless' asymmetric aminohydroxylation. Our group has also recently completed an enantioselective synthesis.[14]

In pursuing a total synthesis of phomopsin B,[15] we synthesized the complete macrocycle and tripeptide side chain with the goal of coupling these advanced intermediates in a highly convergent manner (Chart 1). Unfortunately, the combination of the weak dehydroproline nucleophile with the β-branched carbonyl and acylated amine combined to block this coupling entirely. Conditions that strongly activated the acid resulted in azlactone formation and subsequent epimerization and racemization at C3. Furthermore, the side chain was not able to add to and open this intermediate. Conditions that weakly activated the acid resulted in no reaction. Though we had anticipated these issues at the outset of this strategy, given the myriad peptide coupling agents in general use, it still appeared to be a tractable problem. In particular, this failed reaction colored our retrosynthetic analysis of ustiloxin D.

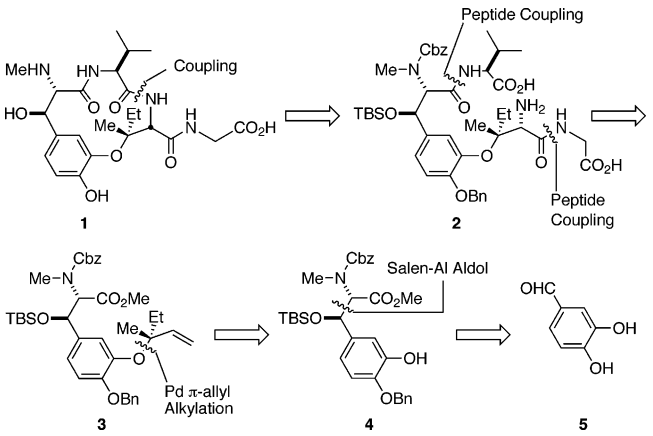

FIGURE 1. Ustiloxin D retrosynthesis.

Results and Discussion

Retrosynthesis. During the development of our synthetic strategy for ustiloxin D, our goal was to use chemistry that would be compatible for application on the more highly functionalized phomopsin system. Thus, it was evident from our studies that the macrocycle needed to be fully formed with the side chain already in place as shown in Figure 1. We envisioned that such closure could be brought about by a novel intramolecular Staudinger ligation[16] or a more conventional peptide coupling strategy. This reduced the problem to linear tetrapeptide **2** that could be formed from the dipeptide precursor **3** by sequential coupling of the glycine side chain and a valine-derived amino acid.

The problem of the tertiary aryl−alkyl ether had previously been addressed using nucleophilic aromatic substitution of a homochiral tertiary alcohol onto a suitably activated arene moiety.[13,15d] This strategy placed stringent demands on the electronics of the arene group, requiring considerable functional group manipulation to elaborate the natural product. To get around this problem, we took advantage of the high functional group tolerance of the Pd asymmetric allylic alkylation.[17] New advances in this methodology led us to believe that this disconnection might be particularly well-suited to deliver the desired aryl−alkyl ether from phenol **4**.

This phenol could in turn be realized by conducting an aldol reaction between a glycine enolate equivalent and a suitably protected 3,4-dihydroxybenzaldehyde **5**. Though most work toward these stereocenters has focused on enantioselective elaboration of an alkene precursor,[13,15c] we chose to use an aldol approach for two

(7) Lin, Y.; Koiso, Y.; Kobayashi, H.; Hashimoto, Y.; Iwasaki, S. *Biochem. Pharmacol*. **1995**, *49*, 1367−1372.
(8) Morisaki, N.; Mitsui, Y.; Yamashita, Y.; Koiso, Y.; Shirai, R.; Hashimoto, Y.; Iwasaki, S. *J. Antibiot.* **1998**, *51*, 423−427.
(9) Lacey, E.; Edgar, J. A.; Culvenor, C. C. J. *Biochem. Pharm.* **1987**, *36*, 2133-2138.
(10) (a) Mutoh, R.; Shirai, R.; Koiso, Y.; Iwasaki, S. *Heterocycles* **1995**, *41*, 9−12. (b) Takahashi, M.; Shirai, R.; Koiso, Y.; Iwasaki, S. *Heterocycles* **1998**, *47*, 163−166.
(11) Laïb, T.; Zhu, J. *Synlett* **2000**, 1363−1365.
(12) Hutton, C. A.; White, J. M. *Tetrahedron Lett.* **1997**, *38*, 1643−1646.
(13) (a) Park, H.; Cao, B.; Jouillié, M. M. *J. Org. Chem.* **2001**, *66*, 7223−7226. (b) Cao, B.; Park, H.; Joullié, M. M. *J. Am. Chem. Soc.* **2002**, *124*, 520−521.
(14) Tanaka, H.; Sawayama, A. M.; Wandless, T. J. *J. Am. Chem. Soc.* **2003**, *125*, 6864−6865.
(15) (a) Stohlmeyer, M. M.; Tanaka, H.; Wandless, T. J. *J. Am. Chem. Soc.* **1999**, *121*, 6100−6101. (b) Woiwode, T. F.; Rose, C.; Wandless, T. J. *J. Org. Chem.* **1998**, *63*, 9594−9596. (c) Woiwode, T. F.; Wandless, T. J. *J. Org. Chem.* **1999**, *64*, 7670−7674. (d) Woiwode, T. F. Ph.D. Thesis, Stanford University, Stanford, California, 2000; Chapters 2 and 3.
(16) (a) Nilsson, B. L.; Kiessling, L. L.; Raines, R. T. *Org. Lett,* **2001**, *3*, 9−12. (b) Nilsson, B. L.; Kiessling, L. L.; Raines, R. T. *Org. Lett.* **2000**, *2*, 1939−1941. (c) Soellner, M. B.; Nilsson, B. L.; Raines, R. T. *J. Org. Chem.* **2002**, *67*, 4993−4996.
(17) Trost, B. M.; Toste, F. D. *J. Am. Chem. Soc.* **1999**, *121*, 4545−4554.

SCHEME 1

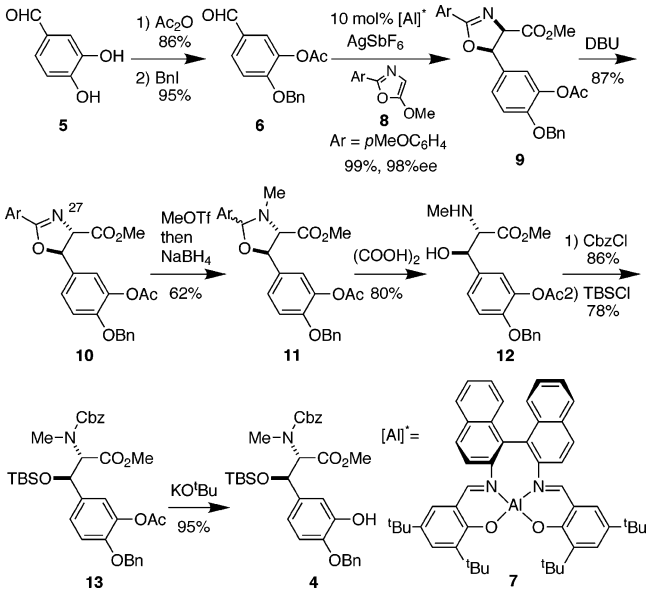

reasons. First, our aldol would produce a *cis*-oxazoline product, more appropriate for the syn relationship of the phomopsin system. However, facile base-mediated isomerization is capable of producing the *trans*-oxazoline, the desired stereochemistry for the anti configuration found in the ustiloxins. Thus, this transformation would be compatible for both molecular scaffolds. Second, the product oxazoline serves as a masked N-methylated amino alcohol that could be revealed at the appropriate time.

Salen−Al Aldol. Our studies toward ustiloxin D were initiated with the differential protection of the hydroxyl groups of commercially available 3,4-dihydroxybenzaldehyde (Scheme 1). The only conditions that gave selectivity were to employ 2.5 equiv of strong base to deprotonate both phenols followed by reaction with 1.2 equiv of acetic anhydride. The acetyl group was allowed to equilibrate between the two potential phenolates eventually acylating the more basic C3 hydroxyl of **5**. For the 4-position, we needed a more robust protecting group that would persist until a final global deprotection. Silyl ethers were inappropriate because upon deprotection of the acetate, concomitant migration of a TBS group between the C3 and C4 hydroxyls was observed. Other efforts involving stable ethereal linkages amenable to fluoride deprotection (such as SEM[18]) were later found to be incompatible with metal-mediated reactions. The ethylene glycol substructure likely chelates to the metal center, attentuating its activity. Though its deprotection conditions would not be useful in the context of the phomopsin B synthesis, benzyl protection was finally settled upon, and after optimization, a 95% yield of **6** was obtained.

This set the stage for the first asymmetric reaction, namely, Evans' Salen−Al aldol[19] between benzaldehyde **6** and the glycine-enolate equivalent **8** (Scheme 1). Although there was no precedent for this reaction using an electron-rich aldehyde, the sluggish reactivity was

(18) SEM: 2-(trimethylsilyl)ethoxymethyl.
(19) Evans, D. A.; Janey, J. M.; Magomedov, N.; Tedrow, J. S. *Angew. Chem., Int. Ed.* **2001**, *40*, 1884−1888.

TABLE 1. Methylation and Reduction of Oxazoline 10

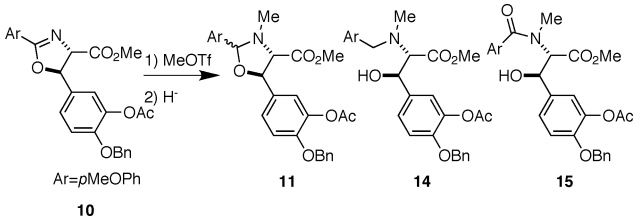

10 **11** **14** **15**

reaction conditions	**10** (%)	**11** (%)	**14** (%)	**15** (%)
$NaBH(OAc)_3$/EtOH	7	33[a]		51
$NaBH(OAc)_3/CH_2Cl_2$	4	6	49	9
$NaBH_4$/EtOH	0	42	13	29
$NaBH_4/CH_2Cl_2$	0	46	21	0
$NaBH_4/CH_2Cl_2$−satd $NaHCO_3$	6	62	24	0
K-selectride/THF	8	55	0	4

[a] This number is a combined yield of **11** and **14**.

circumvented by increasing the catalyst loading from 5 to 10 mol % and rigorously removing all traces of water to deliver 99% yield and 98% ee of *cis*-oxazoline **9**. DBU-catalyzed isomerization set the correct stereochemistry for ustiloxin D to provide **10** in 87% yield and 7% recovery of starting material as a thermodynamic ratio.

In addition to oxygen and nitrogen installation, the oxazoline served a dual purpose as a vehicle to functionalize the N27-nitrogen to an *N*-methylamine. Using the combination of methyl trifluoromethanesulfonate followed by in situ reduction produced the *N*-methyloxazolidine as an inseparable mixture of diastereomers.[20] Though the methylation step was well precedented,[21] many conditions for the reduction were screened to optimize the yield and are summarized in Table 1. In addition to the desired N-methylated oxazolidine, we also observed formation of an overly reduced *N*,*N*-dialkylamino alcohol **14** and methylated hydrolysis product **15**. To minimize side products, sodium borohydride was used as part of a biphasic mixture of saturated sodium bicarbonate solution and dichloromethane. It is likely that the transient *N*-methyloxazolinium ion and sodium borohydride preferentially dissolve in the aqueous layer and undergo reaction. The resulting uncharged product migrates to the organic layer away from the hydride-rich environment, preventing over-reduction. Control of the relative rates of reduction vs hydrolysis was used to minimize production of the benzamide **15**. This was accomplished by using faster reducing agents ($NaBH_4$ vs $NaBH(OAc)_3$) in more activating solvents (water vs ethanol). Mild oxalic acid conditions were sufficient to open the aminal and deliver the desired *N*-methylamino alcohol **12** in 80% yield.

Pd π-Allyl Asymmetric Allylic Alkylation. The next major synthetic hurdle was the asymmetric allylic alkylation to form the chiral ether. Work done by the Trost group had established that Pd π-allyl species undergo nucleophilic attack at the secondary carbon in preference to the primary carbon to deliver chiral tertiary centers over secondary ones.[17] This selectivity presumably arises

(20) (a) Gant, T. G.; Meyers, A. I. *Tetrahedron* **1994**, *50*, 2297−2360. (b) Wilson, S, R.; Mao, D. T.; Khatri, H. N. *Synth. Commun.* **1980**, *10*, 17−23. (c) Nordin, I. C. *J. Heterocycl. Chem.* **1966**, *3*, 531−532. (d) Barmer, B. A.; Meyers, A. I. *J. Am. Chem. Soc.* **1984**, *106*, 1865−1866.
(21) Schmidt, U.; Siegel, W. *Tetrahedron Lett.* **1987**, *28*, 2849−2852.

TABLE 2. Comparison of Yield and Selectivity of Asymmetric Allylic Alkylation Using Tertiary Carbonate 16 over 1 h and Primary Carbonate 17 over 10 h

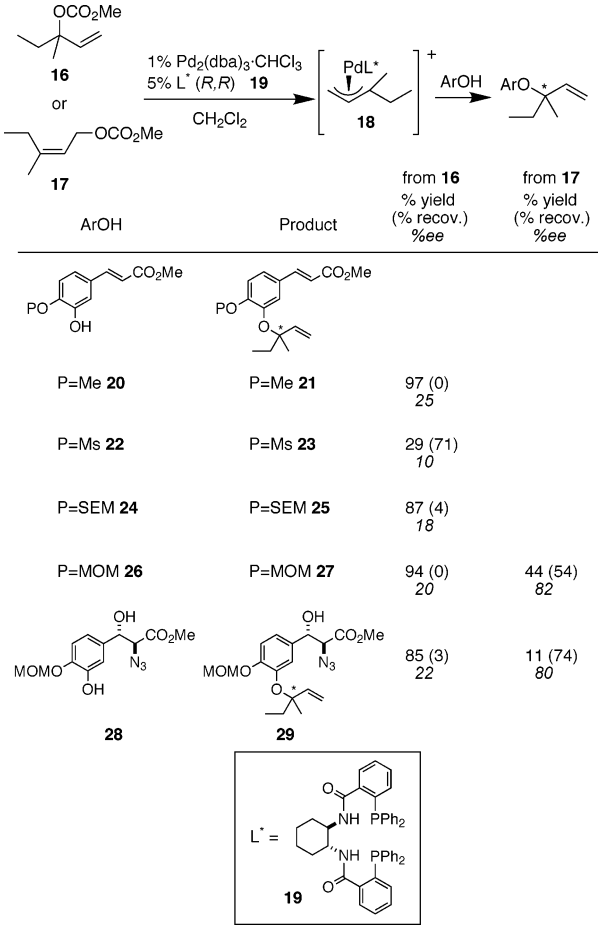

from the greater carbocation-like character of the more highly substituted carbon center following ionization by the Pd(0) metal. However, we were unsure if we would be able to make the extension to form quaternary centers. Such a transformation specifies alkylation at a tertiary carbon over a primary one via a Pd π-allyl species such as **18** (Table 2). Model studies were used to evaluate the viability of this transformation as part of the ustiloxin D synthetic plan. As **18** can be accessed from ionization of either methyl carbonates **16** or **17**, we sought to understand if either of these two precursors provided an advantage over the other.

The results from Table 2 demonstrated that the desired regiochemical outcome was realized every time using all manner of π-allyl precursors, Pd(0) sources, and ligands. More interesting was the divergent conversion and enantioselection observed using each of the two π-allyl precursors. In the presence of 1 mol % $Pd_2(dba)_3{\cdot}CHCl_3$ and 5 mol % (*R*,*R*) ligand **19** in dichloromethane, phenol **26** and tertiary carbonate **16** reacted to give 94% of the desired coupled product when the reaction was stopped immediately after complete phenol consumption (~1 h). By contrast, the primary carbonate **17** underwent a much slower reaction, proceeding to only 44% conversion over 10 h. At this point, if **16** were added to this reaction vessel, complete and near-instantaneous conversion to the desired ether was observed. Stereoselectivity was also affected, as reactions making use of tertiary carbonate **16** delivered unsatisfactory asymmetric induction (10−20% ee) whereas **17** gave ethers in ~80% ee.[22]

With this preliminary data in hand, we tried to take advantage of the improved enantioselectivity of the primary carbonate system and improve conversion. We had reason to believe that the poor yields stemmed from slow Pd-mediated carbonate ionization to produce the active π-allyl cation. In the event that **16** was used, an excess of the electrophile was required (5 equiv) to ensure that the coupled ether did not compete with the **16** as a π-allyl precursor. Over the course of the reaction, all 5 equiv of the tertiary carbonate was consumed, with the generated π-allyl cation predominantly decomposing to a diene via β-hydride elimination. However, even when a single equivalent of **17** was reacted using 20 mol % Pd catalyst loading, no more than 50% consumption was ever observed. For many systems, olefin coordination of the π-allyl precursor to the metal center can be rate-limiting.[23] In such instances, reducing the sterics and improving the electronics can alleviate slow turnover. Though the trisubstituted nature of **17** could not be changed, its electronics could be adjusted to favor precoordination. When a ligand such as an olefin forms π bonds with a metal center, the ligand's HOMO (π orbital) is thought to donate its electrons to the metal center's LUMO (d orbitals). If ionization ensues, however, a significant portion of precoordination is dedicated to back-bonding. In this case, the metal HOMO (d orbital) interacts with the allylic carbonate LUMO (π^* orbital). To improve this latter HOMO−LUMO match, electron-withdrawing groups were added to the π-allyl precursor,[24] as presented in Table 3.

To arrive at the required phenol **4**, the free amine and the hydroxyl group of **12** were sequentially protected and the acetate group was removed using potassium *tert*-butoxide in methanol/THF to deliver the free phenol **4** in 62% over three steps. To enhance conversion, catalyst loading was increased to 10 mol % $Pd_2(dba)_3{\cdot}CHCl_3$ and 50 mol % (*R*,*R*) ligand **19** with primary carbonates reacted for 10 h and tertiary carbonate **16** reacted for 1 h. Leaving groups known to enhance ionization relative to the methyl carbonate such as trichloroethyl (Troc) or trifluoromethyl carbonate and phosphates were reacted with a lack of success similar to the primary methyl carbonate. On the outside chance that slow nucleophilic attack was inhibiting reaction progress of the primary carbonate, we constructed carbonate **34**, envisioning that Pd-mediated ionization would release a proximal phenolate better situated to attack and improve conversion. Unfortunately, we did not observe any change in yield. Taken together, we concluded that effective coordination of the trisubstituted olefin was blocked by steric factors that were impossible to overcome.

We then turned our attention back to the tertiary carbonate system, seeking to increase the enantioselectivity. Lower temperatures appeared to stop the catalyst, as a reaction at −78 °C reduced the yield to 15% of desired ether **30**. Other strategies aimed at increasing

(22) As measured by analytical HPLC using a Chiralpak AD chiral column.

(23) Trost, B. M.; Crawley, M. L. *Chem. Rev.* **2003**, *103*, 2921−2943 and references contained therein.

(24) Trost, B. M.; Toste, F. D. *J. Am. Chem. Soc.* **2000**, *122*, 11262−11263.

TABLE 3. Asymmetric Allylic Alkylation Using Various π-Allyl Precursors with Phenol 4

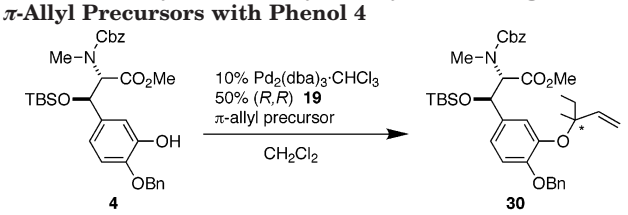

Entry	π-allyl precursor	% yield
1	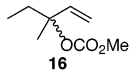 **16**	78
2	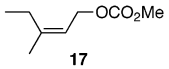 **17**	10
3	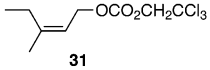 **31**	24
4	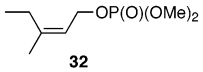 **32**	No Reaction
5	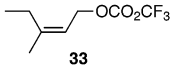 **33**	No Reaction
6	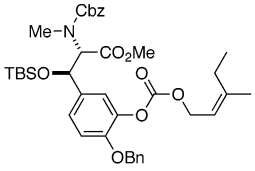 **34**	15

the rate of $\pi-\sigma-\pi$ interconversion[17] (vide infra) through the use of additives such as TBAF, $N(Bu)_4Cl$, $N(Bu)_4I$, or acetic acid were ineffective in raising enantioselection in model systems (data not shown). Last, a screen of various solvents proved to be fruitless, delivering only lower yields and enantioselectivity across a range of model systems. Unfortunately, we were unable to determine the reaction's enantioselectivity using substrate **4**, as the resulting diastereomers were inseparable by chiral HPLC.

We next sought to hydrolyze the C8 ester (Scheme 2). When Cbz-protected secondary amine **30** was subjected to a mild excess of LiOH, free acid **35** was isolated in only 13% yield. Most disturbing to our synthetic plan was the observation of epimerized *N*-methylamine **36** and eliminated cinnamate **37** in 19 and 14% yields, respectively. Lithium hydroperoxide, LiBr/DBU, KO^{t}Bu/DMSO, KO^{t}Bu/H_2O/THF, NaI/pyridine, and TMSI/CH_3CN gave similar myriad products or no reaction at all. In an attempt to relieve some of the steric issues associated with the N-methylated carbamate,[25] we next considered preserving the *trans*-oxazoline until after methyl ester hydrolysis. As an evaluation of this route, we exposed methyl ester **10** to LiOH. To our surprise, we only isolated the deacetylated phenol **40** in 54% yield and a minor compound that was identified as benzamide **39** that was isolated in 18%. We postulate that once the methyl ester is hydrolyzed it spontaneously decarboxylates to deliver **39**. A similar reaction profile was observed using LiOOH and aqueous K_2CO_3. The unprecedented sensitivity to aqueous base of this oxazoline would have important implications in later transformations (vide infra). Smaller nucleophiles such as $LiAlH_4$ also reacted poorly with **10**, delivering the alcohol in 26% yield.

Around this time, the Joullié group published their synthesis of ustiloxin D.[13b] Over the course of this work, they successfully hydrolyzed a C8 ethyl ester. In contrast to our system, which had an α-Cbz-protected secondary amine, the Joullié group had before them an α-Cbz-protected primary amine. In agreement with earlier work,[26] we concluded that LiOH first deprotonates the free N−H of the carbamate. This prevents epimerization and elimination via abstraction of the α-proton because the requisite vicinal dianion is too unstable to form. The excess base can only saponify the ethyl ester. The decomposition that was observed in *N*-methyl carbamate **30** can be attributed to the greater acidity of its α-proton, as there is no N−H proton to first abstract.

These hydrolysis studies gave us three key points to consider: (1) The sterics of a Cbz-protected secondary amine are not compatible with hydrolysis of the C8 ester. (2) An abstractable proton is required on the N27 amine to prevent epimerization at C9. (3) The oxazoline is unstable to aqueous base. Taken together, the best time to saponify the methyl ester would be immediately after the oxazoline was opened to the *N*-methylamino alcohol and before it would be protected as a benzyl carbamate.

We returned to *cis*-oxazoline **9** and discovered that in the presence of anhydrous K_2CO_3 we could effect both isomerization and deacetylation in one step to produce *trans*-phenol **40** in 95% yield (Scheme 3). Etherification was accomplished using 5 mol % $Pd_2(dba)_3$·$CHCl_3$, 25 mol % (*R*,*R*) ligand **19**, and 3 equiv of tertiary carbonate **16** to afford product **41** in 81% yield and 27% de with 15% recovered starting material. Though we had evidence that the primary carbonate **17** produced a more enantioselective reaction in model systems (vide supra), we observed <10% conversion with **17**. We did not confirm the absolute stereochemistry at this juncture and relied upon the predictive model described by the Trost group to assign the (2*R*)-configuration to ether **41a**.[17] However, upon completion of the synthesis and comparison with natural ustiloxin D (vide infra) it became evident that the palladium coupling had proceeded with opposite stereoinduction to predominantly give (2*S*)-ether **41b**.

Asymmetric Sharpless Dihydroxylation. Olefin **41** contains structural motifs that had each been studied individually by the Sharpless group as substrates for asymmetric dihydroxylation.[27] These studies detailed improved selectivity using the $(DHQD)_2PYR$ and $(DHQD)_2PHAL$ ligands,[28] so we pursued dihydroxylations

(25) Similar difficulties with hydrolysis of an ester with an α-*N*-methylated carbamate were observed by: Boger, D. L.; Patane, M. A.; Zhou, J. *J. Am. Chem. Soc.* **1994**, *116*, 8544−8556.

(26) McDermott, J. R.; Benoiton, N. L. *Can. J. Chem.* **1973**, *51*, 2555−2561.

(27) Kolb, H. C.; VanNieuwenhze, M. S.; Sharpless, K. B. *Chem. Rev.* **1994**, *94*, 2483−2547.

(28) (a) Vanhessche, K. P. M.; Sharpless, K. B. *J. Org. Chem.* **1996**, *61*, 7978−7979. (b) Wang, Z.-M.; Zhang, X.-L.; Sharpless, K. B. *Tetrahedron Lett.* **1993**, *34*, 2267−2270. (c) Crispino, G. A.; Jeong, K.-S.; Kolb, H. C.; Wang, Z.-M.; Xu, D.; Sharpless, K. B. *J. Org. Chem.* **1993**, *58*, 3785−3786.

SCHEME 2

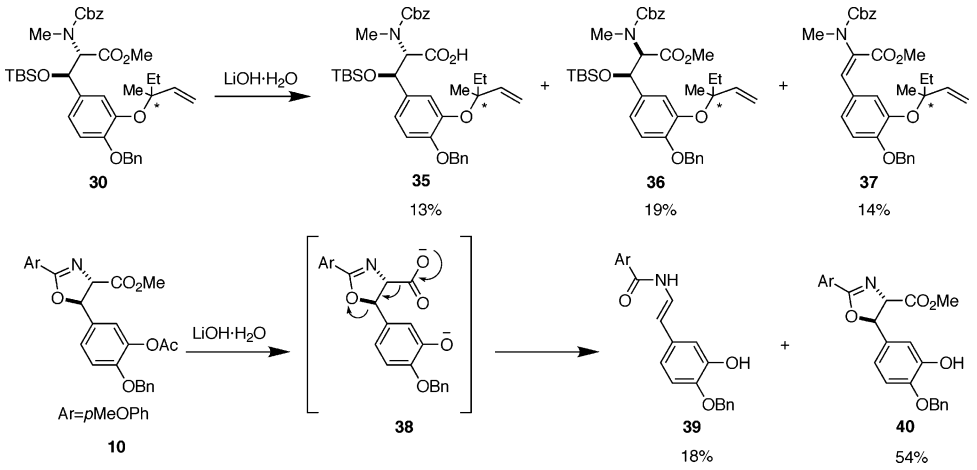

SCHEME 3

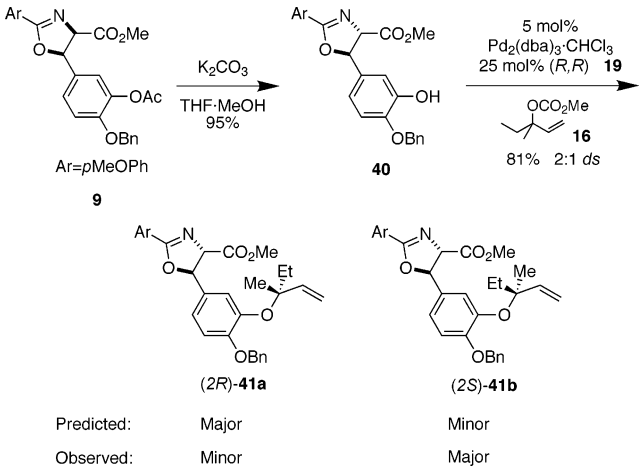

using both ligands. Additionally, to prevent oxazoline decarboxylation we employed a more weakly basic aqueous solution using 2 equiv of $NaHCO_3$/1 equiv of K_2CO_3 rather than the typically prescribed 3 equiv of K_2CO_3. This modification slowed hydrolysis of the intermediate osmate ester such that increased catalyst loading and extended reaction times at room temperature were required to raise conversion to ~75%.

The dihydroxylation reaction produced a complex mixture of four diastereomers (two from Pd etherification and two from dihydroxylation), so evaluation of the reaction diastereoselectivity was very difficult, particularly because **42a/42c** and **42b/42d** behaved chromatographically like enantiomers, each pair eluting as a single peak by reverse-phase C18 analytical HPLC. Because the dihydroxylation selectivity is a function of both the catalyst and the substrate, the selectivities for (2*R*)-**41a** and (2*S*)-**41b** are different (matched and mismatched substrates). These details are more cogently illustrated in Figure 2. The selectivity for the chiral π-allyl palladium reaction is expressed as the mole fraction of (2*R*)-**41a**, x. The mole fraction of (2*S*)-**41b** can be expressed as $(1 - x)$. In a similar manner, the mole fraction of (2*R*,3*S*)-**42a** produced from (2*R*)-**41a** is expressed as y, (mole fraction of (2*R*,3*R*)-**42b** is $(1 - y)$) and the mole fraction of (2*S*,3*S*)-**42d** produced from (2*S*)-**41b** is expressed as z (ratio of (2*S*,3*R*)-**42c** is $(1 - z)$).

Since we do not know which set of diastereomers elute first by HPLC, two interpretations are possible. If pseudoenantiomers (2*R*,3*S*)-**42a** and (2*S*,3*R*)-**42c** elute first and pseudoenantiomers (2*R*,3*R*)-**42b** and (2*S*,3*S*)-**42d** elute second (case 1), the following is true:

$$\frac{\text{peak area 1}}{\text{peak area 2}} = \frac{xy + (1-x)(1-z)}{x(1-y) + (1-x)z} \qquad \text{case 1}$$

xy: mole fraction of (2*R*,3*S*)-**42a**

$(1 - x)(1 - z)$: mole fraction of (2*S*,3*R*)-**42c**

$x(1 - y)$: mole fraction of (2*R*,3*R*)-**42b**

$(1 - x)z$: mole fraction of (2*S*,3*S*)-**42d** (1)

On the other hand, if (2*R*,3*S*)-**42a** and (2*S*,3*R*)-**42c** are the latter eluting isomers, the equation is as follows:

$$\frac{\text{peak area 1}}{\text{peak area 2}} = \frac{x(1-y) + (1-x)z}{xy + (1-x)(1-z)} \qquad \text{case 2} \quad (2)$$

We needed to solve the equation for the two unknowns y and z, y being the selectivity of the correct ustiloxin D (2*R*,3*S*)-**42a** isomer from compound (2*R*)-**41a** (minor product) and z being the selectivity of the C2-epimer of ustiloxin D (major product). Thus, two data sets are needed for the determination. The first set of peak areas was obtained from the analysis of products of dihydroxylation using racemic substrate **41** that was generated by using a racemic ligand for the π-allyl palladium reaction. In this case, $x = (1 - x) = 0.5$. The second set of peak areas was obtained from a dihydroxylation reaction using substrate **41** that was generated stereoselectively by using ligand (*R*,*R*)-**19**. In this case, chiral HPLC established that $x = 0.365$ and $(1 - x) = 0.635$. The necessary data were collected, and y and z values were calculated from the above equations for both case 1 and case 2 and compiled in Table 4.

In case 1, all selectivities are greater than 0.5, implying that the DHQD ligands preferentially form the desired (3*S*)-**42** compounds, an outcome predicted by the Sharpless mnemonic. In case 2, all selectivities are less than 0.5, implying that the reaction is running counter to expectation. On the basis of the reliability of this mnemonic and subsequent confirmation by total synthesis, we believe that our reaction falls into case 1, in which

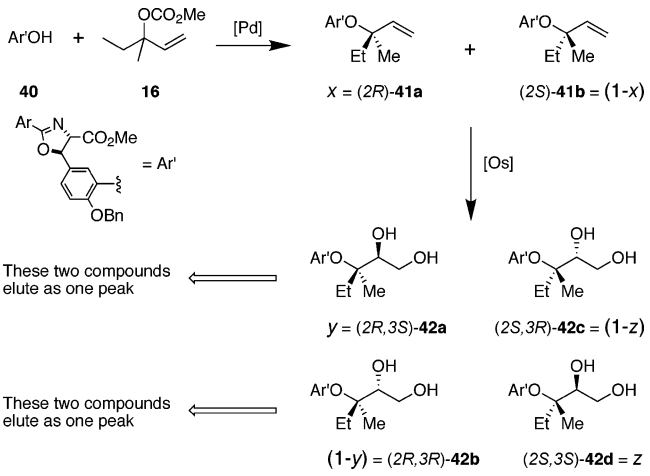

FIGURE 2. Determination of diastereoselectivies of the dihydroxylation reaction.

TABLE 4. Selectivities of Dihydroxylation Reaction Using $(DHQD)_2PHAL$ and $(DHQD)_2PYR$

		$(DHQD)_2PHAL$		$(DHQD)_2PYR$	
		area 1	area 2	area 1	area 2
$x = 0.365$		54.28	45.72	37.08	62.92
$x = 0.5$		57.25	42.75	46.81	53.19
case 1	y (de)	0.5375 (7.5%)		0.8285 (66%)	
	z (de)	0.6825 (37%)		0.8923 (78%)	
case 2	y (de)	0.4625 (−7.5%)		0.1715 (−66%)	
	z (de)	0.3175 (−37%)		0.1077 (−78%)	

pseudoenantiomers (2*R*,3*S*)-**42a** and (2*S*,3*R*)-**42c** elute first and pseudoenantiomers (2*R*,3*R*)-**42b** and (2*S*,3*S*)-**42d** elute second. $(DHQD)_2PYR$ is therefore the more selective ligand. Its dihydroxylation on the ustiloxin D substrate **41a** is 66% de, and the selectivity for the C2-epimer **41b** is 78% de, indicating that we were working with a mismatched pair.

Macrocycle Closure. The secondary alcohol resulting from dihydroxylation next needed to be converted to an azide (Scheme 4). Earlier intermediates demonstrated that first protecting the primary alcohol followed by an activation/displacement protocol was unsuccessful. It is likely that the doubly allylic oxygenation renders the electrophilic center of interest too electron-rich for effective S_N2-displacement (data not shown). To this end, we chose to oxidize the primary alcohol and couple the glycine side chain prior to the azide displacement. A two-step oxidation using TEMPO[29]/NaClO[30] followed by sodium chlorite gave the acid in excellent yield (99%), and BOP[31] coupling of the glycine *tert*-butyl ester proceeded rapidly to produce amide **44** in 88% yield (Scheme 4). Despite the strong azide nucleophilicity, preliminary studies had indicated that the neopentyl center mandated a highly active trifluoromethanesulfonate to furnish any substituted product at all (data not shown). Optimized conditions reacted 3 equiv of triflic anhydride with **44**. Though conversion proceeded slowly over 10 h, exposure of the purified triflate **45** to anhydrous LiN_3[32] in DMPU[33]

SCHEME 4

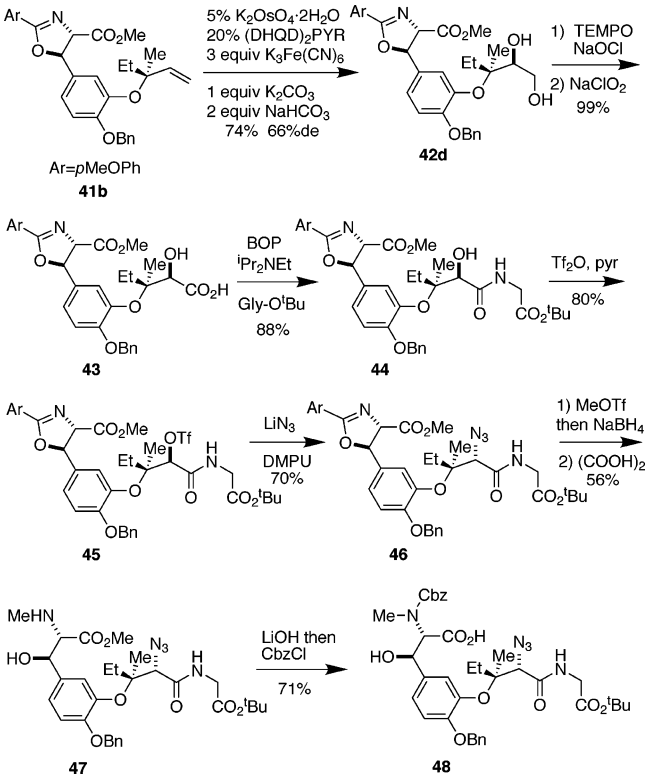

for 24 h gave the azide in 56% yield over two steps. It should be noted that displacements using NaN_3 or LiN_3 in other solvents were significantly less effective. Because the potential existed for oxirane-assisted double inversion at C3, we attempted to effect diastereomer separation by analytical HPLC. Though this work proved to be inconclusive, given the stability of trifluoromethanesulfonate **45** to SiO_2 chromatography and favorable comparison with natural ustiloxin D upon completion of the synthesis, we believe that assisted double displacement does not occur to any significant extent.

Next, the oxazoline protecting group was opened to reveal the *N*-methylamino alcohol. Methyl triflate followed by sodium borohydride provided the intermediate diastereomeric oxazolidines in 83% yield. This was followed by mild acid treatment to unmask the free amine. As expected, since amine **47** was not protected as a carbamate, careful reaction with 3 equiv of LiOH at 0 °C selectively hydrolyzed the methyl ester. As soon as the methyl ester had been fully consumed, 3 equiv of Cbz-Cl was added to convert the intermediate *N*-methylamine to Cbz-protected *N*-methylamino acid **48** in 71% yield. Our mechanistic hypothesis as to the kinetics of ester hydrolysis was borne out as neither epimerization at C9 nor elimination was observed. Furthermore, the glycine *tert*-butyl ester was untouched by these relatively gentle saponification conditions.

At this point, we began studies toward closing the macrocycle. The diverse functionality in **48** demanded mild conditions, and so we turned to the Staudinger ligation, a reaction that uses triphenylphosphine to

(29) TEMPO: 2,2,6,6-tetramethyl-1-piperidinyloxy, free radical.
(30) de Nooy, A. E. J.; Besemer, A. C.; van Bekkum, H. *Synthesis* **1996**, 1153−1174.
(31) BOP: benzotriazol-1-yloxy-tris(dimethylamino)-phosphonium hexafluorophosphate.
(32) Thompson, C. F.; Jamison, T. F.; Jacobsen, E. N. *J. Am. Chem. Soc.* **2001**, *123*, 9974−9983.
(33) DMPU: 1,3-dimethyl-3,4,5,6-tetrahydro-2(*H*)-pyrimidinone.

SCHEME 5

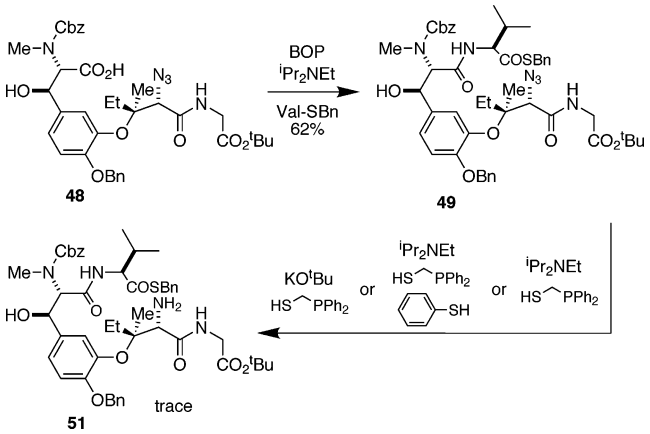

couple an N-terminal azide with a thioester to deliver an amide bond.[16,34] Though we had not found any examples taking place in an intramolecular context to produce macrolactams, we felt that this ligation could be advantageous. The necessary reagent for an intramolecular variant of the Staudinger ligation would require a phosphine and a thiol linked via a methylene unit. Such a reagent could mediate ring contraction from a 16-membered thio-lactone to a more strained 13-membered lactam, in the process taking advantage of preorganization to introduce ring strain in a stepwise fashion. Second, since we introduce the C3 nitrogen as an azide, its direct conversion to an amide would save steps.

The valine thiobenzyl ester was successfully coupled using BOP reagent in 62% yield (Scheme 5). Compound **49** was added slowly via syringe pump to 20 equiv of linked diphenylphosphinomethane thiol and $^{i}Pr_2NEt$ at <1 mM in THF. It was envisioned that the thiol of the linked compound would first undergo thioester exchange followed by iminophosphorane formation. Ring contraction would then give the desired macrocycle. Unfortunately, other than recovered starting material, only a trace quantity of amine **51** was observed. This indicates that phosphine-mediated azide reduction was occurring faster than thioester exchange. This was not unexpected since it is well-documented that branching at the C-terminus slows thioester exchange considerably in native chemical ligations.[35] To increase the rate of thioester exchange, we tried adding (1) benzenethiol,[36] a nucleophilic acylation catalyst, and (2) a phosphine-thiolate linker, generated in situ from ^{t}BuOK/**50**. However, neither of these strategies delivered the desired lactam. Furthermore, standard peptide coupling using PyAOP, BOP, HATU,[37] or BEP[38] on the amino acid derived from **49** did not yield any macrocycle either. Since β-branching of the hydroxyisoleucine may have been incompatible with the steric demands of the macrocycle transition state, we moved our disconnection to the N7−C8 junction.

SCHEME 6

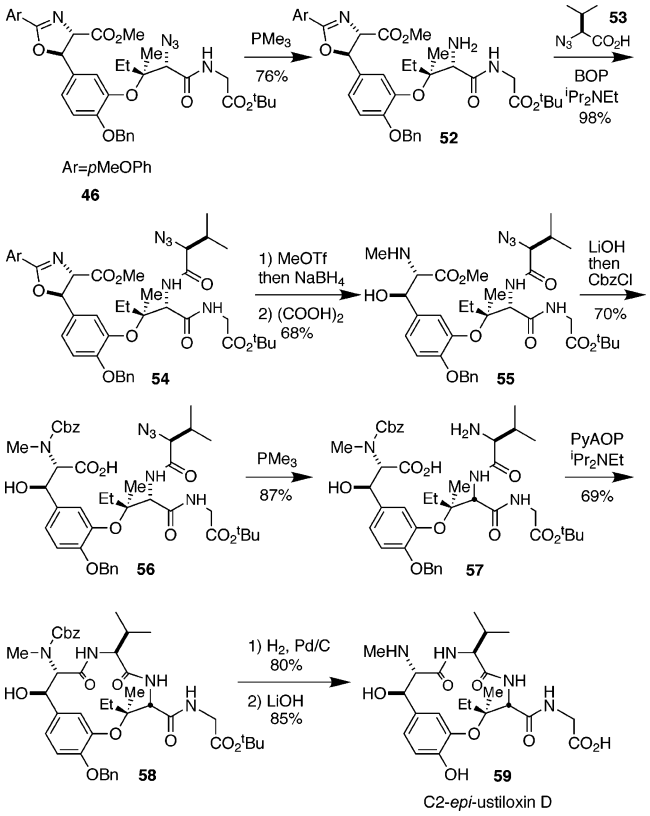

Azide **46** was reduced in 76% yield using PMe_3 followed by quantitative BOP coupling of azido valine[39] **53** (Scheme 6). The methylation/reduction sequence followed by treatment with oxalic acid produced *N*-methylamino alcohol (68%). Elaboration to the azido acid **56** using LiOH and then CbzCl proceeded as before in 70% yield. Though Staudinger conditions were once again unable to close the macrocyle, **56** could be reduced to the amino acid. When reacted using PyAOP at high dilution in DMF, **57** cyclized in good yield to the desired macrolactam **58**. A strong solvent dependence was observed with no macrocycle obtained using dichloromethane.

Earlier results had demonstrated that sufficiently acidic conditions were capable of eliminating the benzylic hydroxyl across C9−C10 (data not shown). We were therefore reluctant to deprotect the *tert*-butyl ester in this way. However, our struggles to hydrolyze the hydroxytyrosine methyl ester led us to believe that basic hydrolysis of the glycinyl ester would be feasible. This prediction was realized when hydrogenolysis of benzyl and Cbz groups were first conducted in 80% yield. Next, 10 equiv of LiOH at room temperature was sufficient to saponify the *tert*-butyl ester and give the final product **59** in 85% yield.

Though **59** matched the expected mass by MS, its analytical HPLC retention time differed significantly from a natural sample of ustiloxin D (Figure S1, see Supporting Information). Deprotected **59** eluted as a 10:1 mixture with only the minor constituent coeluting with natural ustiloxin D at 14.15 min. When we compared ^{1}H NMR in D_2O, not only did the spectra not overlay but

(34) Saxon, E.; Bertozzi, C. R. *Science* **2000**, *287*, 2007−2010. (b) Saxon, E.; Armstrong, J. I.; Bertozzi, C. R. *Org. Lett.* **2000**, *2*, 2141−2143.

(35) Hackeng, T. M.; Griffin, J. H.; Dawson, P. E. *Proc. Natl. Acad. Sci. U.S.A.* **1999**, *96*, 10068−10073.

(36) Dawson, P. E.; Churchill, M. J.; Ghadiri, M. R.; Kent, S. B. H. *J. Am. Chem. Soc.* **1997**, *119*, 4325−4329.

(37) HATU: *O*-(7-azabenzotriazol-1-yl)-*N,N,N′,N′*-tetramethyluronium hexafluorophosphate.

(38) BEP: 1-ethyl-2-bromopyrdinium tetrafluoroborate.

(39) Lundquist, IV, J. T.; Pelletier, J. C. *Org. Lett.* **2001**, *3*, 781−783.

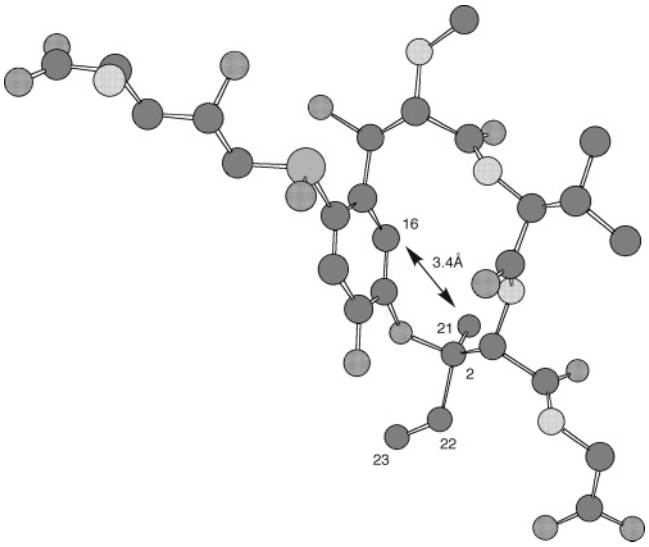

FIGURE 3. Crystal structure of ustiloxin A.

several key peaks varied by >0.1 ppm.[40] The complementary upfield shifts of the C16 aromatic and C21 methyl protons and downfield shifts of the C22 and C23 ethyl protons prompted us to examine the X-ray crystal structure of ustiloxin A (Figure 3). Ustiloxin A differs from ustiloxin D by virtue of a chiral sulfoxide appended at C12 (Chart 1). Its crystal structure indicated that there was only 3.4 Å separating the C16 aromatic proton and the C21 methyl group.[1a] If an inversion of C2 stereochemistry had occurred, this result could be verified by NOE studies. Saturating the C16 proton resonance of natural ustiloxin D led to the observation of an NOE at the C21 methyl but not at the ethyl C22 or C23. When the C16 proton resonance of **59** was saturated, the complementary NOE was observed at the C22 and C23 ethyl group but not at the C21 methyl group. Since our synthetic strategy did not provide any opportunity to epimerize at C2, we concluded that the Pd asymmetric allylic alkylation had proceeded counter to the stereochemical outcome predicted by the model. Such an outcome is not without precedent.[41]

Synthesis of Ustiloxin D. We returned to phenol **40** (Scheme 7), and using 2 mol % $Pd_2dba_3{\cdot}CHCl_3$ and 6 mol % enantiomeric (*S*,*S*) ligand **60** afforded a 2:1 mixture of **41**, with the desired isomer (*R*)-**41a** making up the major product in 71% yield. Dihydroxylation followed by two-step oxidation of the primary alcohol and BOP coupling of the glycine *tert*-butyl ester proceeded in 66% yield over four steps. Our first synthesis of epi-ustiloxin D **59** had seen the 2:1 selectivity at C2 changed to 10:1 by the end of the synthesis. Thus, it appeared as though the diastereomeric epi-C2 stereochemistry was more compatible with ensuing reactions than was the correct C2 isomer. As such, we were especially concerned that lower conversions would be observed in the ensuing activation and displacement of the secondary alcohol using a mixture containing the correct C2 isomer as the major constituent. Much to our gratification, no such reduction in yield occurred. The azide **63** was successfully reduced and coupled to Boc-Val in 81% yield over two steps (Scheme 8). Because we would not be conducting a Staudinger ligation to effect macrocyclization, we did not couple azido valine and instead used a more conventional nitrogen protection. The *N*-methylamino alcohol was successfully unmasked, and the deprotection of both the methyl ester and the Boc-amine proceeded in moderate yield. PyAOP macrocyclization proceeded at reduced yield as compared with the analogous C2-epi compound (56 vs 69%). Two-step deprotection completed the synthesis and produced a 2:1 mixture of ustiloxin D **1** and C2-epi ustiloxin D **59**.[42]

SCHEME 7

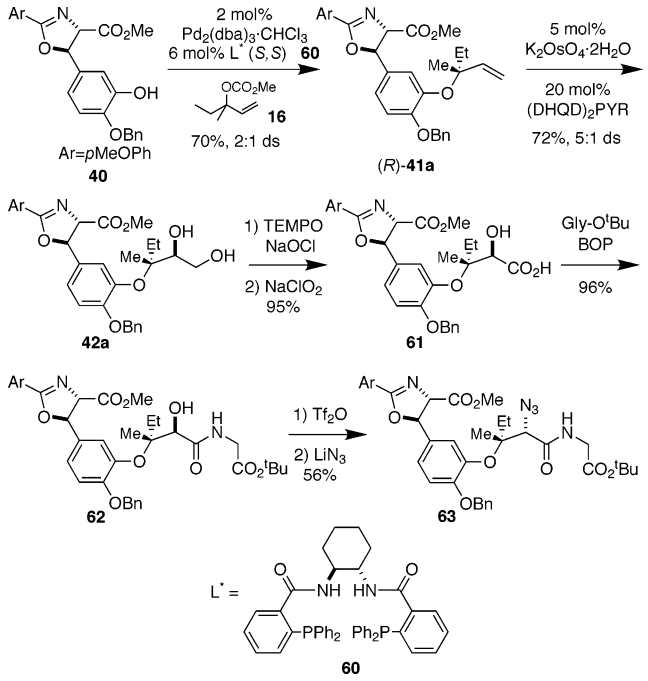

SCHEME 8

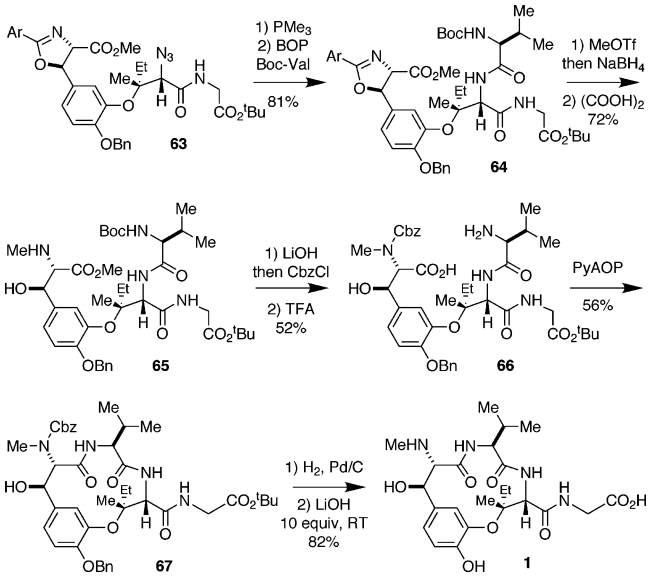

(40) As detailed in Supporting Information for ref 14.

(41) (a) Trost, B. M.; Heinemann, C.; Ariza, X.; Weigand, S. *J. Am. Chem. Soc.* **1999**, *121*, 8667−8668. (b) Trost, B. M.; Gunzner, J. *J. Am. Chem. Soc.* **2001**, *123*, 9449−9450. (c) Trost, B. M.; Gunzner, J. L.; Dirat, O.; Rhee, Y. H. **2002**, *124*, 10396−10415.

(42) We have attributed the discrepancy in ust D **1**:C2-epi ust D **80** using (*R*,*R*) **81** and (*S*,*S*) **24** ligands to reaction diastereoselectivity for each of the two isomers.

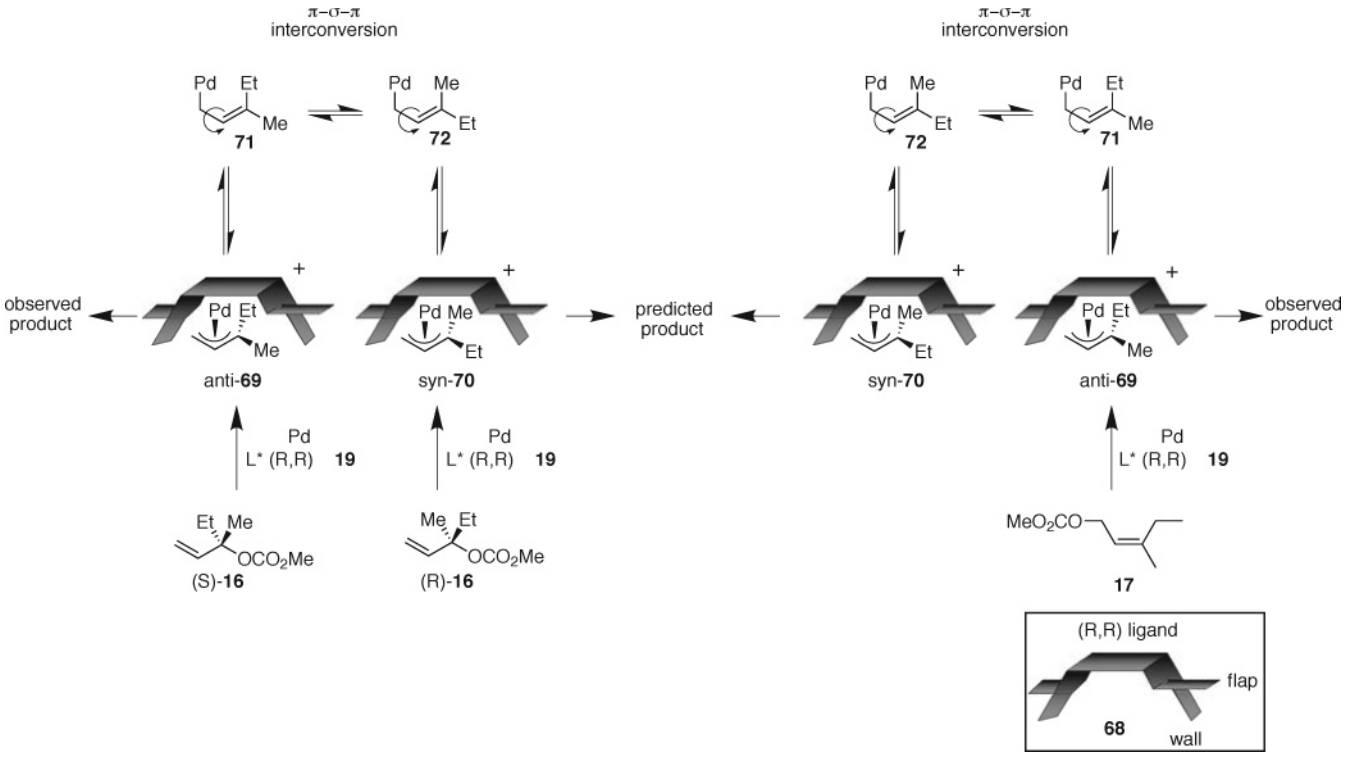

FIGURE 4. Proposed mechannism for the asymmetric allylic alkylation.

Preparative HPLC separated the isomers, and the major constituent proved to be identical to a sample of the natural product by all spectroscopic analyses, including ^{1}H and ^{13}C NMR, HRMS, and specific rotation, as well as by TLC and HPLC analysis. The synthesis was completed with a longest linear sequence of 20 steps and an overall yield of 1.9%.

Mechanistic Description of Asymmetric Allylic Alkylation. An interesting mechanistic question to address is the difference in absolute configuration and the degree of selectivity of the Pd asymmetric allylic alkylation arising from the use of different π-allyl precursors. The chiral space that the (*R*,*R*) ligand defines about Pd can be represented by **68** (Figure 4). Two of the four phenyl groups make up walls, and the other two make up flaps and are arranged with C_2 symmetry. When π-allyl precursors such as (*S*)-**16**/(*R*)-**16** or **17** are ionized by Pd(0) and the (*R*,*R*) ligand **19**, two diastereomeric Pd π-allyl species are formed, *anti*-**69** and *syn*-**70**. These intermediates can then equilibrate via $\pi-\sigma-\pi$ interconversion and alkylate phenol **26** under Curtin−Hammett conditions.[17] Typically, the *anti*-π-allyl is disfavored because this orientation places $A_{1,3}$ strain on the larger substituent.[43] This conformation also places the larger group closer to the ligand wall and the smaller group under the flap. In the case of ustiloxin D, however, the catalytic complex must discriminate between sterically similar methyl and ethyl groups. For this system, it happens that the anti conformation is the more reactive of the two, albeit not by much (2:1 selectivity corresponds to $\Delta\Delta G^{\ddagger} = 0.4$ kcal/mol).

If the rate of $\pi-\sigma-\pi$ interconversion of the π-allyl complex is significantly faster than the ensuing alkylation, it would imply that the alkylation is the enantiodiscriminating step. Were the ustiloxin D system to fall into this kinetic regime, the same enantioselectivity would be observed regardless of the origin of the Pd π-allyl, be it (*S*)-**16**, (*R*)-**16**, **17**, or mixtures thereof. However, using model systems, we observed racemic **16** and **17** to give very different enantioselectivities. This suggests that the ustiloxin D system does not fall into this kinetic regime and alkylates according to an alternate mechanism.

At the other extreme, it is possible that ionization of the π-allyl by Pd is the enantiodiscriminating step. Under this kinetic regime, alkylation of the phenol occurs much faster than $\pi-\sigma-\pi$ interconversion of the π-allyl complex. Thus, the configuration of the π-allyl precursor at ionization is the determining factor of the coupled product's stereochemistry. In such a case, the identity of the ligand bound to Pd would be irrelevant, as the mechanism is essentially proceeding via double S_N2 displacement. Thus, when a racemic mixture of **16** is ionized, a racemic mixture of π-allyl is formed and a racemic product should be observed. By contrast, if **17** is ionized to form a single homochiral π-allyl species, complete enantioselectivity should be the result. Though not in perfect accord, this mechanistic model provides a more accurate description of the observed data, such that ionization of racemic **16** delivers a product of low selectivity (~20% ee) and ionization of **17** delivers high selectivity (~80% ee).

Because conversion was ineffective with the trisubstituted π-allyl precursor **17** (vide supra), studies were restricted to the tertiary carbonate **16**. However, this hypothesis suggests that the only element preventing good selectivity using the tertiary carbonate is its racemic nature. If a single enantiomer (*S*)-**16** could be prepared, its subsequent Pd-mediated ionization would be expected

(43) Trost, B. M.; Lee, C. B. *J. Am. Chem. Soc.* **2001**, *123*, 3671−3686.

to produce a single enantiomeric ether. We are currently pursuing this strategy in the context of the synthesis of phomopsin B.

Conclusion

The total synthesis of (−)-ustiloxin D was accomplished in 20 steps and 1.9% overall yield starting from 3,4-dihydroxybenzaldehyde. We are applying these studies to the more complex phomopsin B system. Three catalytic asymmetric reactions were used to set four of the five stereocenters. The versatility of the aluminum aldol is highlighted by its ability to accommodate the opposite *cis*-hydroxyl stereochemistries of ustiloxin D and phomopsin B. For ustiloxin D, the aldol product *cis*-oxazoline is isomerized to the *trans*-oxazoline to complete the synthesis. For our studies toward phomopsin B, the *cis*-oxazoline will be preserved. The Pd asymmetric allylic alkylation proceeded with low selectivity and good yield using a racemic tertiary π-allyl precursor and proceeded with high selectivity and poor yield using a primary carbonate. Improvement of this transformation is ongoing using a homochiral tertiary carbonate. Our early incorporation of the ustiloxin D side chain should be applicable to the synthesis of phomopsin B and facilitate coupling of the weakly nucleophilic dehydroproline moiety. Finally, though we were unsuccessful in our attempts using the Staudinger ligation to effect macrolactamization of ustiloxin D, we are still pursuing this strategy in the context of phomopsin B.

Acknowledgment. We thank Dr. Yukiko Koiso for providing a sample of natural ustiloxin D. We also thank Professors Evans, Trost, and DuBois and members of their laboratories for helpful advice. This work was supported by the NSF (CHE-9985214) and a Dreyfus Foundation Teacher-Scholar Award to T.J.W. and a NSERC PGS B Award to A.M.S.

Supporting Information Available: Experimental details and analytical data for all new compounds. This material is available free of charge via the Internet at http://pubs.acs.org.

JO048854F